Bioinorganic Chemistry

DOI: 10.1002/anie.201003411

A $\{Cu_2S\}^{2+}$ Mixed-Valent Core Featuring a Cu–Cu Bond**

Stéphane Torelli, Maylis Orio, Jacques Pécaut, Hélène Jamet, Laurent Le Pape, and Stéphane Ménage*

Copper is widely used in biology as a cofactor to fulfil varied functions such as dioxygen activation for aromatic ring oxidations (tyrosinase, catechol oxidase, quercetin 2,3-dioxygenase), alkane oxidations (pMMO), dioxygen carrying (hemocyanins), and H_2O_2 production (galactose oxidase).[1,2] Other peculiar copper structures containing copper–thiolate are more specifically involved in rapid electron-transfer functions. Such sites, called Cu_A, are dinuclear and are found in cytochrome *c* oxidase (CcO)[3–6] and nitrous oxide reductases (N_2OR).[7–10] The resting state is part of the class III family[11] of mixed-valence (MV) species characterized by a fully spin delocalized structure $Cu^{+1.5}Cu^{+1.5}$. Delocalization originates from two S(Cys) bridges and a Cu···Cu separation lying around 2.5 Å. This short intermetallic distance is consistent, as evidenced by extended X-ray absorption fine structure (EXAFS) analysis[12,13] and X-ray diffraction,[3–6] with a Cu–Cu bond. To date, Tolman's $[(L^{i\mathrm{PrdacoS}}Cu)_2(CF_3SO_3)]$ compound ($L^{i\mathrm{PrdacoS}}$ = 1-isopropyl-5-ethylthiolato-1,5-diazacyclooctane) containing a $\{Cu_2N_4S_2\}^+$ core remains the most achieved and structurally characterized MV Cu_A model,[14] although several nonbiologically relevant systems reflecting a MV state have been reported.[15–21] Another intriguing copper site is the Cu_Z center of N_2OR. It consists of a μ_4-sulfido tetranuclear copper cluster that likely alternates between $(Cu^I)_4$ and a partially delocalized MV $(Cu^{II})(Cu^I)_3$ resting state.[22] Delocalization has been shown to be mainly due to the participation of S(3p) orbitals.

Inspired by the Cu_Z center, we prepared copper complexes containing a μ-sulfido ligand. Taking into account mechanistic considerations (that is, substrate fixation at a Cu_2S edge),[23] we investigated the preparation of dicopper species bearing a thiophenolate ligand. Herein, we report the preparation of the first MV copper complex with a $\{Cu_2S\}^{2+}$ motif partially representative of the Cu_Z MV resting state, which contains a Cu–Cu bond and displays a high degree of delocalization. Density functional theory (DFT) calculations were also performed to refine spectroscopic assignments and to confirm unambiguously the Cu–Cu bond.

Reaction of $L^{(Me)S-S}$ (Scheme 1, see the Supporting Information for preparation and characterization) with four equivalents of $[Cu^I(CH_3CN)_4(CF_3SO_3)]$ results, through reductive cleavage of the disulfide bond, in the appearance of an intense violet color that persists over the reaction timescale. Such reactivity applied to aliphatic disulfides has already been reported and leads to the formation of the corresponding dicopper(II) species.[24] Careful addition of diethyl ether into a solution of the compound in either acetone or acetonitrile gave dark X-ray quality crystals (80% yield) of $[L^{(Me)S}Cu_2](CF_3SO_3)_2$ (**1**-$(CF_3SO_3)_2$).[25]

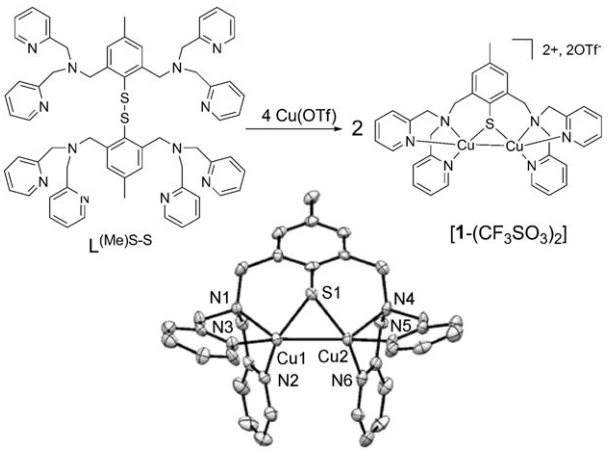

Scheme 1. Top: Synthesis of **1**-$(CF_3SO_3)_2$. Bottom: Representation of the cationic portion of the X-ray crystal structure of **1**-$(CF_3SO_3)_2$ (50% probability ellipsoids; hydrogen atoms omitted for clarity). Selected bond distances [Å] and angles [°]: Cu1–Cu2 2.5762(13), Cu1–S1 2.177(2), Cu2–S1 2.193(2), Cu1–N1 2.127(7), Cu1–N2 1.980(7), Cu1–N3 2.119(6), Cu2–N4 2.115(6), Cu2–N5 2.124(7), Cu2–N6 1.998(7); Cu1-S-Cu2 71.53(9); S1-Cu1-Cu2 53.69(4); S1-Cu2-Cu1 54.78(6). See Supporting Information, Figure S2 for details on the Cu1 and Cu2 coordination polyhedra.

The solved structure shows the presence of a dicationic unit that specifically contains two copper atoms bridged by the thiophenolate-type moiety. The C–S distance for the complex is indeed close to that determined in $L^{(Me)S-S}$ (1.810(8) vs. 1.786(2) Å respectively; Supporting Information,

[*] Dr. S. Torelli, Dr. L. Le Pape, Dr. S. Ménage
Laboratoire de Chimie et Biologie des Métaux, Université Joseph Fourier, CNRS, UMR 5249, CEA, DSV/iRTSV/LCBM Bat K', 17, avenue des Martyrs, 38054 Grenoble Cedex 9 (France)
Fax: (+33) 4-3878-9124
E-mail: stephane.torelli@cea.fr
Dr. M. Orio, Dr. H. Jamet
Equipe de Chimie Théorique, Département de Chimie Moléculaire, Université Joseph Fourier, CNRS, UMR 5250, B.P. 53, 38041 Grenoble Cedex 9 (France)
Dr. J. Pécaut
Laboratoire de Reconnaissance Ionique et Chimie de Coordination—(UMR-E 3 CEA-UJF), SCIB/INAC, CEA-Grenoble, 17, avenue des Martyrs, 38054 Grenoble Cedex 9 (France)

[**] We thank Colette Lebrun for assistance in recording mass spectra and Lionel Dubois for access to the UV/NIR spectrophotometer.

Supporting information for this article, including experimental, instrumental, computational, and crystallographic details, is available on the WWW under http://dx.doi.org/10.1002/anie.201003411.

Figure S1) and the computed C–S(H) values.[26] This comparison reasonably excludes the implication of a phenylthiyl radical. Given these results, the isolation of a MV moiety is reliable. The coordination sphere of each metal also contains the tertiary amine and two pyridine nitrogen atoms, located *cis* to each other (Supporting Information, Figure S2). The coordination polyhedron of the Cu ions having similar shapes and metrics is indicative of a delocalized valence. A striking Cu···Cu distance of 2.576(2) Å is also evidenced. Although this value is slightly out of the range for already reported dinuclear copper complexes exhibiting a Cu–Cu bond, the presence of such an interaction was further confirmed by natural bond order (NBO) calculations (see below). This result represents, to the best of our knowledge, the largest copper–copper bond ever reported for such synthetic systems (usually, the intermetallic distance ranges between 2.39 and 2.45 Å[16–21]).

On the basis of X-ray diffraction data, calculations were undertaken to clarify 1) the degree of delocalization and 2) the relevance of the Cu–Cu bond. Spin population analysis performed at the B3LYP level indicates an equally distributed density (79%) over the two Cu centers together with the bridging sulfur ligand (0.27 for both Cu1 and Cu2, 0.25 for S, Figure 1a), highlighting a fully delocalized $Cu^{+1.5}Cu^{+1.5}$ MV

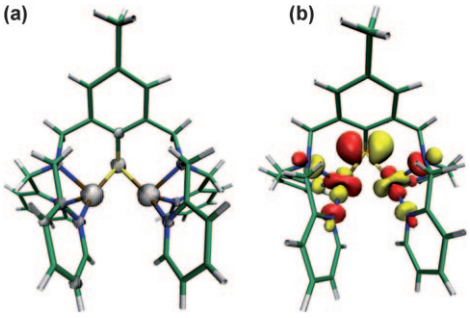

Figure 1. a) Spin-density plot and b) localized SOMO for **1**-$(CF_3SO_3)_2$.

state. The remaining electronic density (21%) is spread over the pyridine rings. Not surprisingly, the singly occupied molecular orbital (SOMO) of **1**-$(CF_3SO_3)_2$ (Figure 1b) displays 60% Cu character and 25% sulfur character featuring the σ antibonding interaction between the Cu($3dz^2$) orbitals and the S(3p) orbital. Contribution of the sulfur atom in the SOMO suggests a nonnegligible degree of covalency for the Cu–S bond.

Independently, NBO analyses from additional single-point calculations (Supporting Information; Table S1) provide direct insight into the Cu–Cu bond evidenced crystallographically. The Wiberg bond index of 0.40 for **1**-$(CF_3SO_3)_2$ is close to the value of 0.50 determined for an in silico model with a Cu···Cu separation of 2.3 Å, which is consistent with a metal–metal bond. A value of 0.19 was also obtained using a model with an intermetallic distance of 3.0 Å, which excludes a Cu–Cu bond. Moreover, an unequivocal picture of the Cu–Cu bonding emerges from the NBO analysis, which clearly identifies a σ 4s3d–4s3d bond between the two copper sites (Figure 2). Note that a similar orbital was found for calcu-

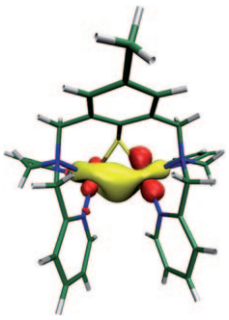

Figure 2. Occupied natural orbital relevant to the Cu–Cu bond resulting from NBO analysis of **1**-$(CF_3SO_3)_2$. Color scheme: Cu brown, S yellow, N dark blue, C light green, and H white.

lations using our complex modeled with the shortest Cu···Cu distance (i.e. 2.3 Å).

The mixed-valence description gained in solid state is also transposable in solution. First, the mass spectrum exhibits prominent peaks at m/z 822 and 336.6, values expected for a mono and di-charged unit respectively, in agreement with calculated isotopic distributions (Supporting Information, Figure S3). Conductivity measurements are also in accordance with a $\{Cu_2S\}^{2+}$ motif (Supporting Information, Figure S4). Second, the EPR spectrum recorded in acetone/toluene exhibits a multiline pattern that can be best simulated with parameters belonging to a highly delocalized $Cu^{+1.5}Cu^{+1.5}$ MV state (Figure 3): $g = (2.218, 2.152, 2.021)$, $A_{Cu1} = (370, 200, 5)$, and $A_{Cu2} = (240, 210, 25)$ in MHz. However, the feature around 320 mT could not be reproduced precisely. Additional experiments indicate substantial solvent dependent behavior that precisely affects this part of the spectrum (Supporting Information, Figure S5). We therefore conclude that this feature is reminiscent to the quality of the glass (possible crystallites and changes in charge distribution by solvation) and not to a disturbance in the electronic delocalization, since the overall pattern of the signal is conserved. The values are in the range of those obtained by DFT calculations: $g_{DFT} =$

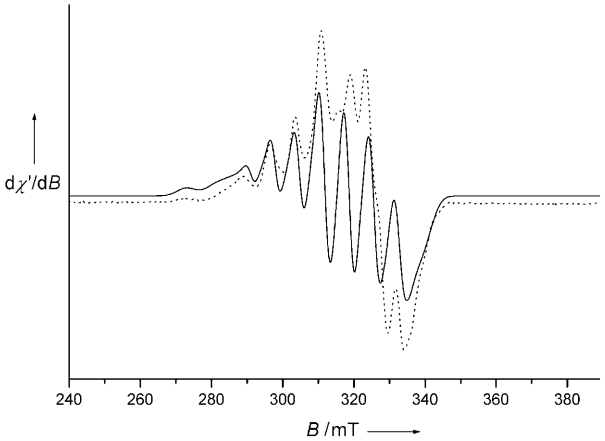

Figure 3. X-band EPR spectrum (9.38838 GHz) of **1**-$(CF_3SO_3)_2$ in acetone/toluene (1:1 v/v, 0.5 mM) at 8 K; modulated amplitude = 1 mT, modulated frequency = 100 kHz, microwave power 1 mW. Dotted line: simulation with parameters given in the text and bandwidths values of 130, 75, and 120 MHz.

(2.138, 2.099, 2.026), $A_1 = (370, 210, 40)$, and $A_2 = (350, 200, 5)$ in MHz. Deviations are not surprising since DFT calculations are based on solid-state structures, whereas EPR simulations relied on frozen solutions.

Third, the electrochemical behavior of **1**-$(CF_3SO_3)_2$ (Figure 4) investigated by cyclic voltammetry in acetone, acetonitrile, or dichloromethane elicited two successive

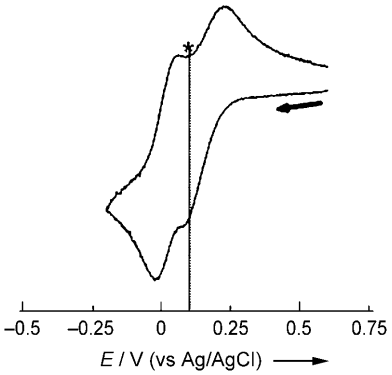

Figure 4. CV curve of **1**-$(CF_3SO_3)_2$ (2.3 mM in CH_3CN) with 0.1 M $Bu_4N(BF_4)$ as supporting electrolyte, Ag/AgCl 3 M as reference electrode, glassy carbon disk as working electrode, and a scan rate of 100 mV s^{-1}. The asterisk denotes the OCP.

reduction waves when starting a higher potential relative to the open circuit potential (OCP, 97 mV). The first, partially reversible wave ($\Delta E_p = 152$ mV, $E_{pa} = 230$ mV, $E_{pc} = 78$ mV, $E_{1/2} = 154$ mV vs. Ag/AgCl) is assigned to the $Cu_2^{II,II}/Cu_2^{II,I}$ process while the second, clearly reversible wave ($\Delta E_p =$ 76 mV, $E_{1/2} = 32$ mV vs. Ag/AgCl) should rely to the $Cu_2^{I,II}/Cu_2^{I,I}$ couple. The insensitivity of the voltammogram to solvent reinforces the hypothesis postulated for the observed EPR behavior in frozen solutions.

The presence of the MV species at the OCP is further confirmed by additional experiments with a rotating-disk electrode (RDE; Supporting Information, Figure S6). The inflexion point observed at the OCP value indicates that the electroactive species present at the electrode can be simultaneously oxidized or reduced. The $E_{1/2}$ values allowed the determination of a comproportionation constant (K_{com}) of 10^2, indicating a nonnegligible thermodynamic stability of the MV form.[28]

Finally, the UV/Vis/NIR absorption spectra of **1**-$(CF_3SO_3)_2$ (Figure 5) exhibits noticeable solvent-dependent features.[29] On the basis of the ε values, these bands are generically assigned to charge-transfer (CT) transitions. They are slightly red-shifted relative to those identified in previously reported Cu_A sites or in $[(L^{iPrdacoS}Cu)_2]^{2+}$, but compare well with some values published for the N_2OR Cu_Z center.[30] The NIR band is the most affected by the nature of the solvent as highlighted by former studies on MV dicopper compounds,[19] stressing to a first approximation an origin from intervalence charge transfer (IVCT).

Time-dependent DFT (TD-DFT) calculations provide clear evidence about the nature of the observed transitions and a reasonable assignment of these bands. The expected

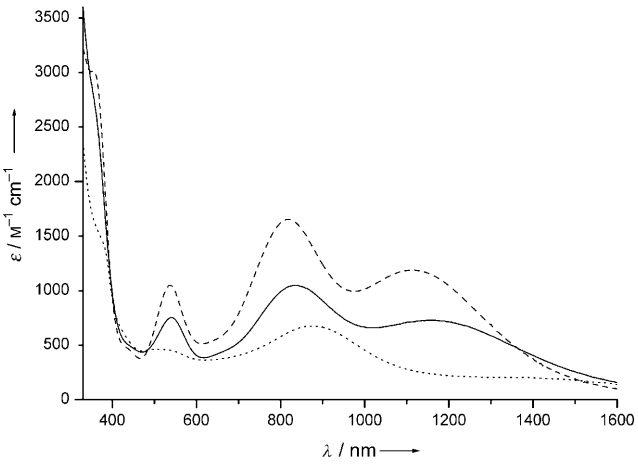

Figure 5. Electronic absorption spectra of **1**-$(CF_3SO_3)_2$ at 25 °C in CH_3CN (dotted), CH_2Cl_2 (solid), and acetone (dashed).

energy values (503 nm, 727 nm, 1009 nm; Supporting Information, Table S2) are in agreement with those for a solution of the complex in acetone (537 nm, 816 nm, 1017 nm). Ligand-to-metal charge transfer (LMCT) bands emerged for the two components observed in the visible region, whereas IVCT (arising from $\Psi \rightarrow \Psi^*$ transition) bands are representative of the NIR absorption (Figure 6).

In conclusion, a MV $\{Cu_2S\}^{2+}$ core has been prepared from reductive cleavage of a disulfide precursor by a Cu^I salt. This represents the first example of a synthetic entity that gathers a

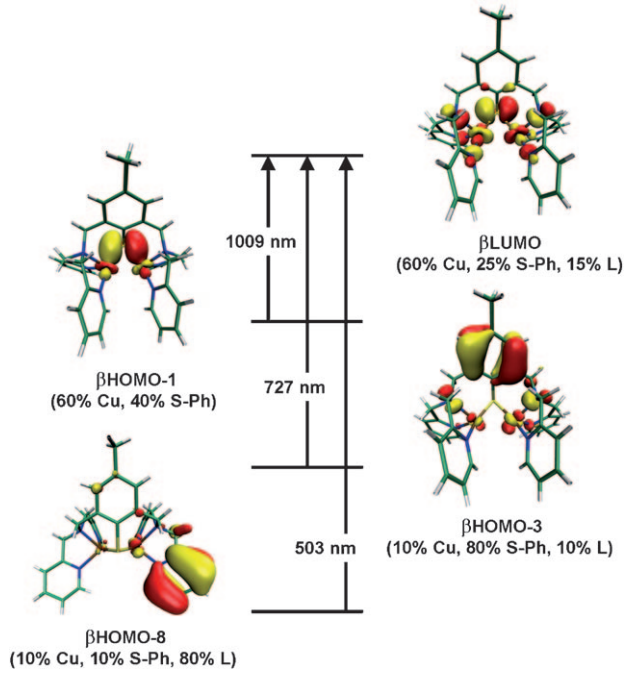

Figure 6. TD-DFT assignment of the calculated transitions for **1**-$(CF_3SO_3)_2$ in acetone. The population of the relevant MOs (HOMO: highest occupied molecular orbital, LUMO: lowest unoccupied molecular orbital) is indicated in parentheses as well as the wavelength of the optical transitions. S-Ph denotes the thiophenolate part of the ligand and L denotes the rest of the ligand.

μ-thiophenolato moiety coordinated to a dinuclear center featuring a Cu–Cu bond. Such a system is partially representative of the sophisticated Cu_Z active site of N_2OR in the sense that it reproduces some of its spectroscopic features and models the Cu-S-Cu edge presumed to be involved in the substrate fixation. Reduction of **1**-$(CF_3SO_3)_2$, or its analogues, could open the prospect for new copper–μ-thiolato species able to perform N_2O reduction,[33–36] and allow structure–reactivity correlations.

Received: June 4, 2010
Revised: August 9, 2010
Published online: September 17, 2010

Keywords: copper · density functional calculations · metal–metal interactions · mixed-valent compounds · oxidoreductases

[1] E. A. Lewis, W. B. Tolman, *Chem. Rev.* **2004**, *104*, 1047 – 1076.
[2] R. Balasubramanian, S. M. Smith, S. Rawat, L. A. Yatsunyk, T. M. Stemmler, A. C. Rosenzweig, *Nature* **2010**, *465*, 115 – 119.
[3] S. Iwata, C. Ostermeier, B. Ludwig, H. Michel, *Nature* **1995**, *376*, 660 – 669.
[4] T. Tsukihara, H. Aoyama, E. Yamashita, T. Tomikazi, H. Yamaguchi, K. Shinzawa-Itoh, R. Nakashima, R. Yaono, S. Yoshikawa, *Science* **1995**, *269*, 1069 – 1074.
[5] M. Wilmanns, P. Lappalainen, M. Kelly, E. Sauer-Eriksson, M. Saraste, *Proc. Natl. Acad. Sci. USA* **1995**, *92*, 11955 – 11959.
[6] E. Kim, E. E. Chufán, K. Kamaraj, K. D. Karlin, *Chem. Rev.* **2004**, *104*, 1077 – 1133.
[7] K. Brown, M. Tegon, M. Prudencio, A. S. Pereira, S. Besson, J. J. G. Moura, I. Moura, M. Tegoni, C. Cambillau, *Nat. Struct. Biol.* **2000**, *7*, 191 – 195.
[8] K. Brown, K. Djinovic-Carugo, T. Haltia, I. Cabrito, M. Saraste, J. J. G. Moura, I. Moura, M. Tegoni, C. Cambillau, *J. Biol. Chem.* **2000**, *275*, 41133 – 41136.
[9] K. Paraskevopoulos, S. V. Antonyuk, R. G. Sawers, R. R. Eady, S. S. Hasnain, *J. Mol. Biol.* **2006**, *362*, 55 – 65.
[10] T. Haltia, Brown, M. Tegoni, C. Cambillau, M. Saraste, K. Matilla, K. Djinovic-Carugo, *Biochem. J.* **2003**, *369*, 77 – 88.
[11] M. R. Robin, P. Day, *Adv. Inorg. Chem. Radiochem.* **1968**, *10*, 247 – 403.
[12] N. J. Blackburn, M. E. Barr, W. H. Woodruff, J. van der Oost, S. de Vries, *Biochemistry* **1994**, *33*, 10401 – 10407.
[13] N. J. Blackburn, S. de Vries, M. E. Barr, R. P. Houser, W. B. Tolman, D. Sanders, J. A. Fee, *J. Am. Chem. Soc.* **1997**, *119*, 6135 – 6143.
[14] R. P. Houser, V. G. Young, W. B. Tolman, *J. Am. Chem. Soc.* **1996**, *118*, 2101 – 2102.
[15] R. R. Gagné, C. A. Koval, T. J. Smith, *J. Am. Chem. Soc.* **1977**, *99*, 8367 – 8368.
[16] D. D. Lecloux, R. Davydov, S. J. Lippard, *J. Am. Chem. Soc.* **1998**, *120*, 6810 – 6811.
[17] D. D. Lecloux, R. Davydov, S. J. Lippard, *Inorg. Chem.* **1998**, *37*, 6814 – 6826, and references therein.
[18] R. Gupta, Z. H. Zhang, D. Powell, M. P. Hendrich, A. S. Borovik, *Inorg. Chem.* **2002**, *41*, 5100 – 5106.
[19] J. R. Hagadorn, T. I. Zahn, L. Que, Jr., W. B. Tolman, *Dalton Trans.* **2003**, 1790 – 1794.
[20] J. Kuzelka, Mukhopadhyay, B. Spingler, S. J. Lippard, *Inorg. Chem.* **2004**, *43*, 1751 – 1761.
[21] S. Kababya, J. Nelson, C. Calle, F. Neese, D. Goldfarb, *J. Am. Chem. Soc.* **2006**, *128*, 2017 – 2029.
[22] P. Chen, I. Cabrito, J. J. G. Moura, I. Moura, E. I. Solomon, *J. Am. Chem. Soc.* **2002**, *124*, 10497 – 10507.
[23] S. Ghosh, S. I. Gorelsky, S. DeBeer George, J. M. Chan, I. Cabrito, D. M. Dooley, J. J. G. Moura, I. Moura, E. I. Solomon, *J. Am. Chem. Soc.* **2007**, *129*, 3955 – 3965.
[24] S. Itoh, M. Nagagawa, S. Fukuzumi, *J. Am. Chem. Soc.* **2001**, *123*, 4087 – 4088.
[25] Crystal data for **1**-$(CF_3SO_3)_2$: $C_{35}H_{33}Cu_2F_6N_6O_6S_3$, $M_r = 970.93$, crystal size 0.50 mm × 0.04 mm × 0.04 mm, monoclinic, space group $P21/n$, $a = 9.4703(7)$ Å, $b = 28.166(3)$ Å, $c = 14.3634(9)$ Å, $\beta = 91.82(5)°$, $V = 3831(5)$ Å^3, $\rho_{calcd} = 1.683\ g\,cm^{-3}$, $Z = 4$, $\mu = 1.357\ mm^{-1}$, $2\theta_{max} = 49.42$, $T = 150(2)$ K, ($\lambda Mo_{K\alpha} = 0.71073$ Å), $F(0,0,0) = 1972$, 16275 reflections collected, 6484 unique, $R_{int} = 0.0470$. The final agreement factors are $R_1 = 0.065$ and $wR2 = 0.1917$ for data with $I > 2\sigma(I)$. CCDC 777283 contains the supplementary crystallographic data for this paper. These data can be obtained free of charge from The Cambridge Crystallographic Data Centre via www.ccdc.cam.ac.uk/data_request/cif.
[26] Y. Fu, B.-L. Lin, K.-S. Song, L. Liu, Q.-X. Guo, *J. Chem. Soc. Perkin Trans. 2* **2002**, 1223 – 1230.
[27] Onsager slope in $CH_3CN = 1352$ (Supporting Information, Figure S6), ESI MS (CH_3CN): $[M-CF_3SO_3]^+ = 822.1$ (Supporting Information, Figure S4).
[28] R. R. Gagné, C. A. Koval, T. J. Smith, M. C. Cimolino, *J. Am. Chem. Soc.* **1979**, *101*, 4571 – 4580.
[29] **1**-$(CF_3SO_3)_2$ in $(CH_3)_2CO$ (λ_{max} [nm] (ε [$M^{-1}cm^{-1}$])): 355 (3150), 537 (1050), 816 (1650), 1017 (1190); in CH_2Cl_2: 365 (3250), 540 (755), 838 (1050), 1185 (720); in CH_3CN : 382 (1600), 510 (465), 875 (675), 1310 (205).
[30] Cu_A (N_2OR) from *A. cycloclastes*:[31] 350 (sh), 481 (5200), 534 (5300), 630 (sh), 780 (2900); Cu_A-soluble binding domain from *P. denitrificans*:[32] 363 (1200), 480 (3000), 532 (3000), 808 (1600); $[(L^{iPrdacoS}Cu)_2]^{2+}$ in CH_3OH: 358(2700), 602(800), 786(sh), 1466 (1200); Cu_Z (N_2OR) from *P. nautica*:[22] 356 (3295), 500 (930), 700 (1455), 638 (3470), 1000 (1760).
[31] C. L. Hulse, B. A. Averill, *Biochem. Biophys. Res. Commun.* **1990**, *166*, 729.
[32] P. Lappalainen, R. Aasa, B. G. Malström, M. Saraste, *J. Biol. Chem.* **1993**, *268*, 26416.
[33] P. Chen, S. I. Gorelsky, S. Ghosh, E. I. Solomon, *Angew. Chem.* **2004**, *116*, 4224 – 4233; *Angew. Chem. Int. Ed.* **2004**, *43*, 4132 – 4140.
[34] J. M. Chan, J. A. Bollinger, C. L. Grewell, D. M. Dooley, *J. Am. Chem. Soc.* **2004**, *126*, 3030 – 3031.
[35] I. Bar-Nahum, A. K. Gupta, S. M. Huber, M. Z. Ertem, C. J. Cramer, W. B. Tolman, *J. Am. Chem. Soc.* **2009**, *131*, 2812 – 2814.
[36] W. B. Tolman, *Angew. Chem.* **2010**, *122*, 1034 – 1041; *Angew. Chem. Int. Ed.* **2010**, *49*, 1018 – 1024.

